Steady State Multiplicities in an Ethylene Glycol Reactive Distillation Column

Amy R. Ciric* and Peizhi Miao

Department of Chemical Engineering, University of Cincinnati, ML 171, Cincinnati, Ohio 45221-0171

A series of homotopic continuation studies are presented that explore steady state multiplicities in a reactive distillation column producing ethylene glycol from ethylene oxide and water. The glycol column has two sets of multiplicities: a three-branch multiplicity that occurs at large values of the holdup volume and a complex switchbacking multiplicity that occurs at small values of the holdup volume. The optimal column has three steady states, and at small holdup volumes, the column can have as many as nine steady states. The computational studies show that the multiplicities are not affected by feed or holdup volume distribution and are not caused by multiple reactions, the temperature dependency of the reaction rate, or the exothermic heat of reaction. The three-branch multiplicity arises from coupling between the bilinear reaction rate and the large volatility differences between the reactants. Analytical results show that the lower turning point of this multiplicity occurs when the oxide feed has been consumed and water begins to accumulate in the vapor boilup streams. The upper turning point of the multiplicity takes place via a series of complex switchbacks that create a second set of multiplicities. This switchbacking multiplicity is more complex, and is influenced by the reactant volatility difference and the kinetic reaction rate constants.

1. Introduction

Reactive distillation occurs when a chemical reaction takes place within the liquid holdup on a distillation tray. This process was first proposed by Backus in 1921, and has since become a popular approach for producing esters and the gasoline oxidant methyl *tert*-butyl ether (MTBE).

A significant amount of effort has been placed on steady state simulation and design of reactive distillation columns. Several methods have been presented for computing a single steady state of a reactive distillation column, including Newton-Raphson methods (Nelson, 1971; Komatsu and Holland, 1977; Carra et al., 1979), modified tri-diagonal methods (Suzuki et al., 1971; Izarraraz et al., 1980; Tierney and Riquelme, 1982; Xu and Chen, 1988), and inside-out algorithms (Venkataraman et al., 1990). Lastly, the homotopic continuation studies of Chang and Seader (1988) are capable of identifying both a single steady state and multiple steady states.

Previous research in reactive distillation design has largely focused upon systems at or near chemical equilibrium. Barbosa and Doherty (1988a,b) have developed residue curve design methodologies for systems involving a single equilibrium-limited chemical reaction. This work is currently being extended to multireaction systems (Ung and Doherty, 1993) and to kinetically limited systems featuring constant Damköhler numbers (Doherty and Buzad, 1992). More recently, Ciric and Gu (1994) have presented an alternative approach to synthesizing reactive distillation columns when chemical reaction equilibrium cannot be assured. Their method identifies the optimal number of trays, holdup volumes, feed tray locations, and reflux ratios by solving a mixed integer nonlinear programming problem.

Relatively little work has been done on the multiplicities and the steady state stability of reactive distillation columns. Pisarenko et al. (1988) showed analytically that a one-product column with reaction confined to the reboiler can have three steady states. Luyben (1993) reported that dynamic simulations of similar systems converged to either a high or low steady state, suggesting that Pisarenko et al.'s observations are correct and that the middle state is unstable. Most recently, Nijhuis et al. (1993) have reported finding steady state multiplicities during the simulation of a two-product MTBE reactive distillation column, and Jacobs and Krishna (1993) observed multiple steady states in the residue curve maps of the MTBE system.

These previous works demonstrated the existence of steady state multiplicities, but did not identify the cause. The objective of this work is to identify steady state multiplicities in an ethylene glycol reactive distillation column and to develop some understanding of their origin. The ethylene glycol process features highly exothermic reactions, temperature-dependent reaction rates, and large volatility differences between components. Each of these features may be a source of multiplicities, and so the ethylene glycol process is an excellent candidate for multiplicity analysis.

A series of computational studies are performed to explore the multiplicities of a column designed by Ciric and Gu (1994). The studies use a problem-specific homotopy that treats the liquid holdup on reactive trays as a homotopy parameter. Varying this homotopy parameter gives a curve that shows the number of steady states as a function of the holdup volume. This homotopy was used to study the effect of feed tray location, holdup volume distributions, multiple reactions, heats of reactions, activation energy, and reactant volatility upon multiplicity. These computational results are combined with analytical arguments to provide a mechanistic explanation of the multiplicities.

2. Ethylene Glycol Reactive Distillation Column

Ciric and Gu (1994) have presented a reactive distillation column for manufacturing ethylene glycol (EG)

* Author to whom correspondence should be addressed. E-mail: aciric@mikado.che.uc.edu.

0888-5885/94/2633-2738$04.50/0

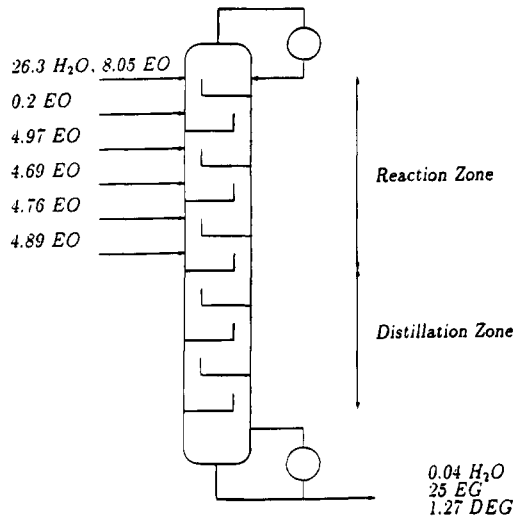

Figure 1. Optimal distributed feed reactive distillation column for ethylene glycol synthesis.

Table 1. Physical Property Data

Antoine Equation and Coefficients:

$$PK_{i,k} = A_{i,1} \exp\left\{A_{i,2}\frac{T_k - A_{i,3}}{T_k - A_{i,4}}\right\} \quad P = [\text{atm}],\ T_k = [\text{K}]$$

component	$A_{i,1}$	$A_{i,2}$	$A_{i,3}$	$A_{i,4}$	T_b (K)
ethylene oxide	71.9	5.72	469	35.9	283.5
water	221.2	6.31	647	52.9	373.2
ethylene glycol	77	9.94	645	71.4	470.4
diethylene glycol	47	10.42	681	80.6	519.0

reaction data	
ethylene glycol production	$r = \exp\{37.0 - (9547.7/T)\}\cdot x_{EO}x_W$ kmol/(m^3 h), $T = [\text{K}]$; $\Delta H = -80$ kJ/mol
diethylene glycol production	$r = \exp\{37.6 - (9547.7/T)\}\cdot x_{EO}x_{EG}$ kmol/(m^3 h), $T = [\text{K}]$; $\Delta H = -13.1$ kJ/mol
heat of vaporization	40 kJ/gmol
column pressure	1 atm

and diethylene glycol (DEG) from ethylene oxide and water via the reactions

$$C_2H_4O + H_2O \rightarrow C_2H_6O_2\ (\text{EG})$$

$$C_2H_4O + C_2H_6O_2 \rightarrow C_4H_{10}O_3\ (\text{DEG})$$

Ethylene glycol is the major product of these reactions, and diethylene glycol is a waste byproduct. Physical property data for these reactions are given in Table 1.

The cost-optimal column is shown in Figure 1. This column contains 10 trays. Reaction and separation occur on trays 5 through 10 in the column, and separation without chemical reaction occurs on trays 1 through 4. Reaction volumes are distributed unevenly between trays 5−10. Water in the amount of 26.3 kmol/h is fed onto the top tray, and a total feed of 27.56 kmol/h of ethylene oxide is distributed among trays 6−10. The distribution of the ethylene oxide feed and the liquid holdup volumes among the reactive trays is given in Table 2.

This column produces no distillate products: instead, the vapor leaving the top tray is condensed completely and recycled. The bottoms boil-up ratio is 0.958, and 26.3 kmol/h of bottoms is produced. The bottoms stream is composed of 95% ethylene glycol, 4.8% diethylene glycol, and 0.2% water. The column produces 25 kmol of ethylene glycol per hour.

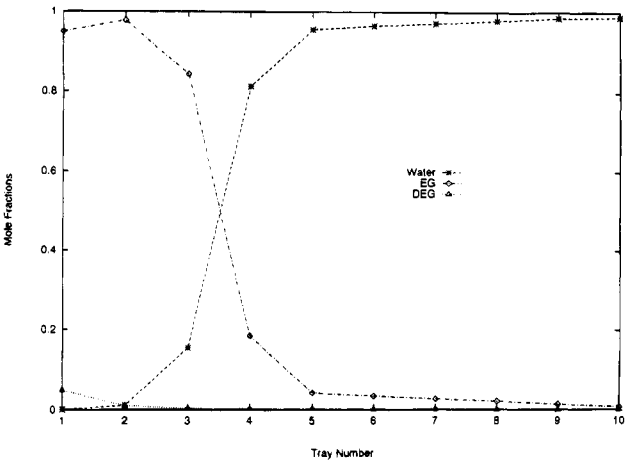

Figure 2. Composition profile within the optimal (base case) ethylene glycol reactive distillation column.

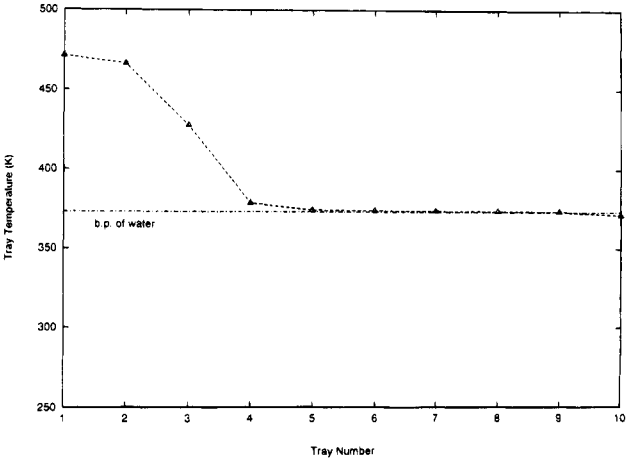

Figure 3. Temperature profile within the optimal (base case) ethylene glycol column.

Table 2. Column Design Data

Oxide Feeds and Reaction Volumes

tray	oxide feed rate (kmol/h)	reaction volume (m^3)
5	4.89	0.551
6	4.76	0.481
7	4.69	0.447
8	4.97	0.371
9	0.2	1.447
10	8.05	0.011

no. of trays	10
column diam	1.3 m
reflux ratio	∞
boil-up ratio	0.958

The composition profile within the column is shown in Figure 2. Notice that there is virtually no ethylene oxide anywhere within the column, and that the reaction zone in the upper portion of the column contains mostly water. This is reflected in the temperature profile (Figure 3). The temperature in the zone is constant and equal to 373 K, the boiling point of water.

The following section will describe a rigorous model of this column. Homotopic continuation methods, described in section 4, will be used to identify steady state multiplicities in the base column. Homotopic continuation methods will also be used to explore how the number and form of the multiplicities are affected by the holdup volume, the feed distribution, holdup volume distribution, heats of reaction, reaction activation energy, and the volatility difference between the feeds.

3. Reactive Distillation Model

The following assumptions are adopted from the work by Ciric and Gu (1994): (1) the vapor and liquid phases are in equilibrium on each tray; (2) the vapor−liquid equilibrium is ideal; (3) the reactions only occur in liquid phase; (4) the liquid phase is homogeneous; (5) the enthalpy of the liquid streams is negligible relative to the heat of vaporization and the heats of reaction; (6) the heat of vaporization and the heats of reaction are constant; and (7) the reactions only occur on the trays within in the reaction zone.

The following indices will be used to model the column:

$i = 1, ..., I$ chemical species in the reactive system

$j = 1, ..., J$ chemical reactions

$k = 1, ..., N$ trays in the column, numbered from bottom to top

The tray $k = 1$ is a partial reboiler operating at a reboil ratio β, and the desired products are taken out here. The tray $k = N$ is followed by a total condenser with an infinite reflux ratio.

The steady state model of the column is given by the material and energy balances, reaction rate equations, and summation equations. The material balance for chemical species i on tray k in the middle of the column is given by

$$F_{i,k} + V_{k-1}K_{i,k-1}x_{i,k-1} + L_{k+1}x_{i,k+1} - L_k x_{i,k} - V_k K_{i,k} x_{i,k} + \sum_j \nu_{i,j}\xi_{j,k} = 0 \quad (1)$$

where $F_{i,k}$ is the feed rate of the chemical species i to the tray k, V_k is the vapor flow rate of tray k, L_k is the liquid reflux off tray k, and $x_{i,k}$ is the mole fraction in the liquid holdup on tray k. In addition, $K_{i,k}$ is the vapor−liquid equilibrium coefficient for component i on tray k, $\nu_{i,j}$ is the stoichiometric coefficient of component i in reaction j, and $\xi_{j,k}$ is the extent of reaction j on tray k. The value of $K_{i,k}$ is calculated from Antoine's equation. It should be noted that the stoichiometric coefficient $\nu_{i,j}$ is positive if the component i is a product of reaction j and negative if the component i is a reactant of reaction j.

The vapor stream V_N off the top tray is totally condensed and returned to the tray:

$$F_{i,N} + V_{N-1}K_{i,N-1}x_{i,N-1} - L_N x_{i,N} + \sum_j \nu_{i,j}\xi_{j,N} = 0 \quad (2)$$

A portion β of the liquid stream leaving the bottom tray is vaporized and fed back to the tray:

$$L_2 x_{i,2} - (1-\beta)L_1 x_{i,1} - V_1 K_{i,1} x_{i,1} + \sum_j \nu_{i,j}\xi_{j,1} = 0 \quad (3)$$

The extent of reaction j is calculated from the kinetic equation

$$\xi_{j,k} = W_k f_j(x_{i,k}, T_k) \quad (4)$$

Here W_k is the liquid holdup volume on tray k and f_j is the kinetic rate of reaction j, written as a function of the tray composition x_{ik} and the tray temperature T_k.

With assumptions 5 and 6, the energy balance for tray k becomes

$$H_{vap}(V_{k-1} - V_k) - \sum_j \Delta H_j \xi_{j,k} = 0 \quad (5)$$

Here, H_{vap} is the heat of vaporization and ΔH_j is the heat of reaction j.

In addition to these material and energy balance equations, the mole fractions of chemical species in each liquid or vapor stream must sum to unity:

$$\sum_i x_{i,k} = 1 \quad (6)$$

and

$$\sum_i K_{i,k} x_{i,k} = 1 \quad (7)$$

Equations 1−7 constitute a tray-by-tray model of the reactive distillation column. This model contains $N(I + J + 3) + 1$ variables: N temperatures T_k, $J\,N$ extents of reactions $\xi_{j,k}$, N liquid streams L_k, N vapor phase streams V_k, $I\,N$ liquid compositions $x_{i,k}$, and the reboil ratio β. There are $N(I + J + 3)$ equations in the model: $I\,N$ material balances, N energy balances, $2N$ summation equations, and $J\,N$ reaction rate expressions. Fixing the reboil ratio removes the degree of freedom, and eqs 1−7 become a square system of nonlinear equations.

The model defined by eq 1−7 is highly nonlinear and may admit more than one solution. The objective of this work is to test for any multiplicities and identify their sources. This will be accomplished with the homotopic continuation method described in the next section.

4. Overview of Homotopy Continuation

The reactive distillation model presented in the previous section is nonlinear and may have multiple solutions. Some of these solutions can be identified with homotopic continuation methods (Alexander and Yorke, 1978; Wayburn and Seader, 1987).

A linear homotopy is constructed from two vector functions and a parameter:

$$\mathbf{H}(\mathbf{x},\lambda) = \lambda\mathbf{f}(\mathbf{x}) + (1-\lambda)\mathbf{g}(\mathbf{x}) = \mathbf{0} \quad (8)$$

Here, $\mathbf{f}(\mathbf{x})$ is the original nonlinear vector function with one or more roots, $\mathbf{g}(\mathbf{x})$ is a simpler vector function with one unique root, and λ is the homotopy parameter. When $\lambda = 0$, the solution of the homotopy lies at the unique root of $\mathbf{g}(\mathbf{x}) = \mathbf{0}$. Solutions of $\mathbf{f}(\mathbf{x}) = \mathbf{0}$ correspond to solutions of the homotopy when $\lambda = 1$. Consequently, there is a path between the unique solution of $\mathbf{g}(\mathbf{x}) = \mathbf{0}$ and solutions of $\mathbf{f}(\mathbf{x}) = \mathbf{0}$.

All solutions to the homotopy equation $\mathbf{H}(\mathbf{x},\lambda) = \mathbf{0}$ define a homotopy curve in $(\mathbf{x}, \lambda)$ space. Multiple solutions of the equation $\mathbf{f}(\mathbf{x}) = \mathbf{0}$ are detected when the homotopy curve turns back upon itself and crosses the line $\lambda = 1$ more than once.

Differential arc-length continuation methods are commonly used to track a homotopy curve (Wayburn and Seader, 1987). This approach differentiates the algebraic homotopy equations with respect to an arc length, yielding a set of partial differential equations. Integrating these equations gives the homotopy curve. Homotopy curves can also be generated with dynamic reparametrization. This approach does not require differentiating the homotopy equations, but instead generates each point on the curve by solving a system of nonlinear equations. At each iteration of the approach, a new

point on the homotopy curve is generated by making a fixed size step in the variable with the largest rate of change. Initially, fixed-size steps are made along λ, the homotopy parameter. As a turning point is approached, the change of some critical variable x^* with each step in λ will begin to increase. Taking fixed steps along this critical variable rather than λ ("reparametrization") allows one to track the homotopy curve around a turning point, generating a curve like the one shown in Figure 4.

5. Ethylene Glycol Homotopy

In this section we present a homotopy model of the base case design described in Section 2. The homotopy is constructed by setting the vector function $\mathbf{f}(\mathbf{x})$ equal to the full model of the reactive distillation column, given by eqs 1−7. The simpler vector function $\mathbf{g}(\mathbf{x})$ is taken as a model of a nonreactive distillation column with the same number of trays, reflux ratio, feed tray locations, and boil-up ratio as the original reactive distillation column. This nonreactive model is constructed by replacing the term $W_k f_j(x_{ik},T_k)$ with 0, so that the extents of reaction within the column are identically equal to zero.

The homotopic system of equations is

$$F_{i,k} + V_{k-1}K_{i,k-1}x_{i,k-1} + L_{k+1}x_{i,k+1} - L_k x_{i,k} - V_k K_{i,k} x_{i,k} + \sum_j \nu_{i,j}\xi_{j,k} = 0 \quad (9)$$

$$F_{i,N} + V_{N-1}K_{i,N-1}x_{i,N-1} - L_N x_{i,N} + \sum_j \nu_{i,j}\xi_{j,N} = 0 \quad (10)$$

$$L_2 x_{i,2} - (1-\beta)L_1 x_{i,1} - V_1 K_{i,1} x_{i,1} + \sum_j \nu_{i,j}\xi_{j,1} = 0 \quad (11)$$

$$\xi_{j,k} - \lambda_1 W_{kfj}(x_{i,k},T_k) = 0 \quad (12)$$

$$H_{vap}(V_{k-1} - V_k) - \sum_j \Delta H_j \xi_{j,k} = 0 \quad (13)$$

$$\sum_i x_{i,k} = 1 \quad (14)$$

$$\sum_i K_{i,k} x_{i,k} = 1 \quad (15)$$

When λ_1 equals 1, these equations model the reactive distillation column described in section 2. This system of equations may have more than one solution. When λ_1 equals 0, the extents of reaction are identically equal to 0, and eqs 9−15 describe a nonreactive column. Since the vapor−liquid equilibrium is ideal and there is one product, this nonreactive column will have a single unique steady state. Consequently, the homotopy curve will pass through the line $\lambda_1 = 0$ once and only once.

This homotopy was chosen over a Newton homotopy (Chang and Seader, 1988) or a fixed-point homotopy (Kuno and Seader, 1988) because it provides physically significant information everywhere along the path. Notice that $\lambda_1 W_k$ can be interpreted as a holdup volume. If $\lambda_1 = 1$, the holdup volume equals the design specification; if $\lambda_1 = 0.8$, the holdup volume is 80% of the design specification. Thus by adding the homotopy parameter λ_1, we can obtain the solutions of the reactive distillation system at different holdup volumes.

This work used the optimization model developed by Ciric and Gu (1994) as the basis of the homotopy study.

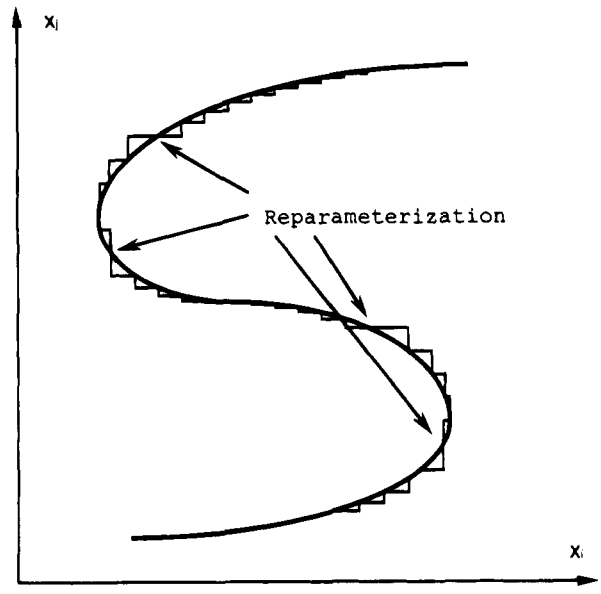

Figure 4. Steps and turning points during dynamic reparametrization.

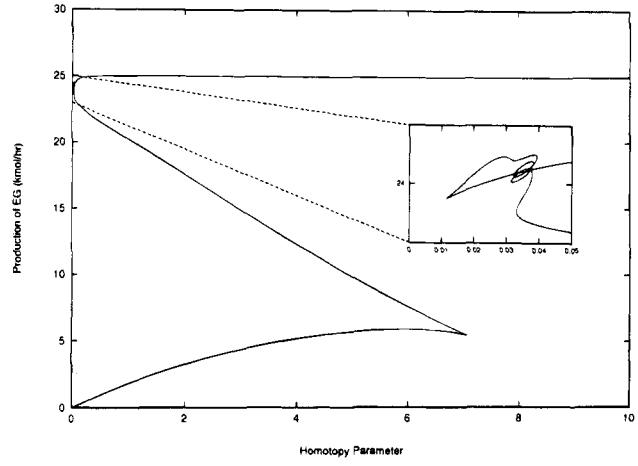

Figure 5. Ethylene glycol production as a function of the homotopy parameter in the base case column.

All degrees of freedom (boil-up ratio, reflux ratio, number of trays, hold-up volume, feed rates) in the original problem were fixed at their optimal values, transforming the optimization code into a Newtonian equation solver. This transformation is explained in more detail in the Appendix. This Newtonian solver was used as a subroutine in a GAMS program (Brooke et al., 1988) that generated the homotopy curve by dynamic reparametrization.

It should be noted that one cannot guarantee that this homotopy will generate all solutions to eqs 1−7, or that isolas do not exist. The use of dynamic reparametrization does, however, allow for some multiplicities to be identified.

6. Base Case Design

The number of steady states that can occur within the base case column was determined with the problem-specific homotopy described in the previous section. The production of ethylene glycol ($C_2H_6O_2$) as a function of the homotopy parameter λ_1 for the base case design is shown in Figure 5. The column has two types of multiplicities. There is a large-scale three-branch multiplicity with a cusplike turning point between the intermediate and low branches. There is also a complex

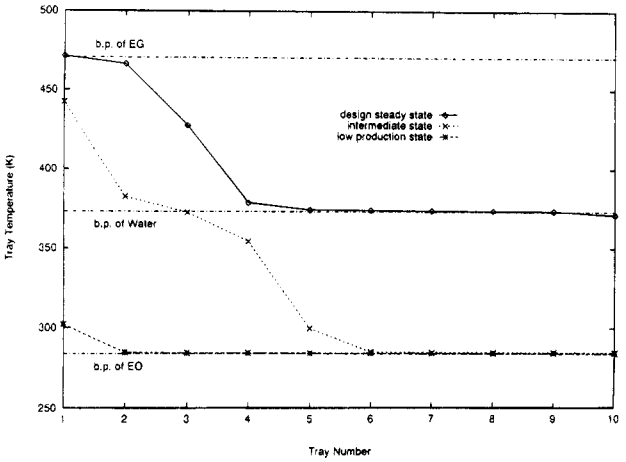

Figure 6. Temperature profile at the three steady states of the base case column.

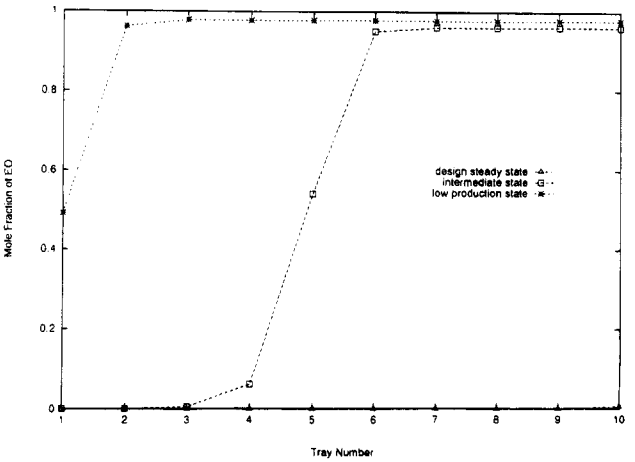

Figure 7. Ethylene oxide concentration profile at the three steady states of the base column.

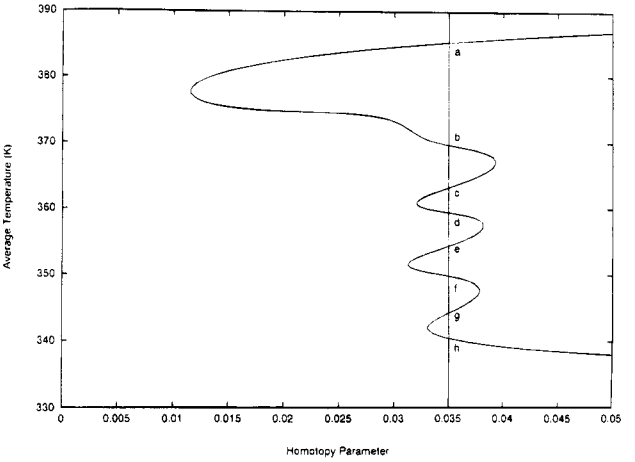

Figure 8. Average temperature versus homotopy parameter in the base case colum: illustration of switchbacking multiplicities.

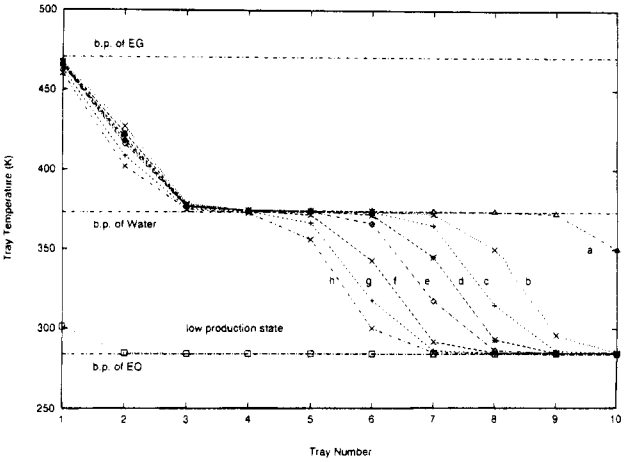

Figure 9. Temperature profiles in the steady states of the base case column in the switchbacking region, $\lambda_1 = 0.035$.

small-scale "switchbacking" multiplicity nestled within the transition between the upper and intermediate branches of the large-scale multiplicity.

These results show that the base case column ($\lambda_1 = 1$) has three different steady states. The upper steady state occurs at the optimal operating condition described in section 2. The intermediate steady state produces about 20 kmol/h of ethylene glycol, and the lower steady state produces about 2 kmol/h of ethylene glycol. The column temperature and oxide concentration profiles for all three states are shown in Figures 6 and 7.

At the upper or design state, the temperature throughout the reaction zone (trays 5−10) equals the boiling point of water. The temperature rises steadily throughout the separation zone, reaching the boiling point of ethylene glycol on the bottom tray. There is no significant concentration of ethylene oxide anywhere within the column. At the intermediate state, the temperature profile throughout most of the reaction zone equals the boiling point of ethylene oxide. The temperature within the separation zone rises steadily, reaching a point midway between that of boiling points of water and glycol on the bottom tray. Although the reaction zone is full of ethylene oxide, there is no ethylene oxide in the bottoms product.

At the lower state, the temperature profile throughout the entire column is flat, and the temperature everywhere equals the boiling point of ethylene oxide. The column is full of ethylene oxide, there is little reaction, and most of the oxide fed to the column leaves in the bottom product. Closer scrutiny of the homotopy data shows that the column is full of oxide everywhere along the lower branch of the homotopy curve. The cusplike turning point occurs when there is no oxide in the bottoms product.

A series of switchbacking multiplicities are also exhibited at small holdup volumes ($\lambda_1 \sim 0.035$). These steady state multiplicities are most easily observed in the average column temperature (Figure 8). Clearly, at some small holdup volumes there can be as many as nine different steady states. The temperature and composition profiles for the steady state at $\lambda_1 = 0.035$ are shown in Figures 9 and 10. Notice that in state a the temperature profile within the reaction zone is nearly flat, with a slight drop-off on tray 10. The temperature in the zone equals the boiling point of water, indicating that trays 3−9 are full of water. During the transition from state a to state b, the temperature on trays 3−7 has stayed constant, while the temperature on tray 8 has dropped slightly. At the same time, the temperature on trays 9 and 10 has dramatically dropped from 373 K, the boiling point of water, to 280 K, the boiling point of ethylene oxide. This indicates that, during the transition, the composition on trays 9 and 10 have gone from nearly pure water to nearly pure ethylene oxide. Figures 9 and 10 show that the transitions to other steady states are also accompanied by similarly dramatic composition transitions, isolated on one or two trays. Each state seems

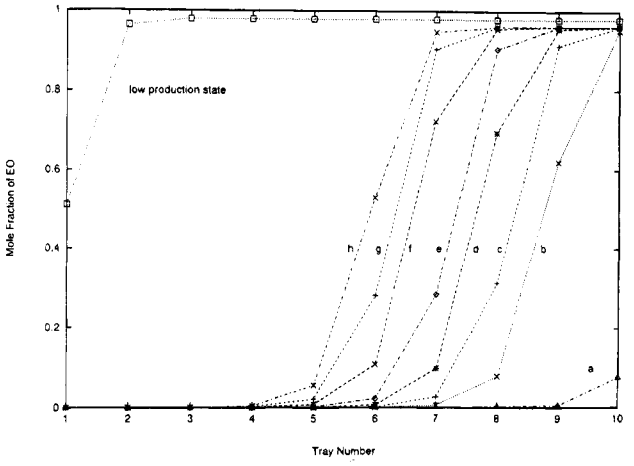

Figure 10. Ethylene oxide composition profiles for the steady states of the base case column in the switchbacking region, $\lambda_1 = 0.035$.

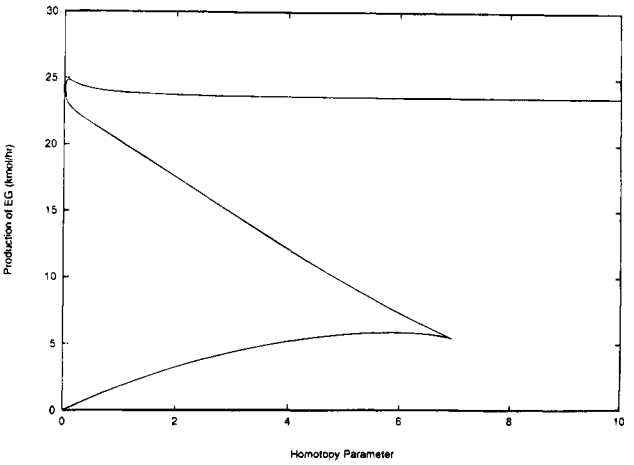

Figure 11. Homotopy curve for a two-feed column: ethylene glycol production versus λ_1.

to represent the transition of one tray from water to ethylene oxide, with little change occurring on other trays.

7. Source of Multiplicities

There are several possible sources of the multiplicities described in the previous section. This section will use homotopic continuation to explore the effect of (a) distributed feeds, (b) distributed holdup volumes, (c) the heat of reaction, (d) the number of reactions, (e) the activation energy, and (f) the volatility difference between the reactants as sources of multiplicity.

7.1. Distributed Feeds. The effect of the distributed ethylene oxide feed was tested by replacing the distributed system with a single ethylene oxide feed located on tray 5. In this modified column, all of the 27.56 kmol/h ethylene oxide is fed to tray 5, rather than distributed between trays 5−10.

Repeating the homotopy on λ_1 produces a new homotopy curve (Figure 11). The major difference between this case and the base case is a reduction of 1 kmol/h in ethylene glycol production rate along the upper branch of the homotopy curve.

7.2. Distributed Holdup Volumes. In the base case design, the reactive holdup volume is unevenly distributed among the reacting trays. The effect of this uneven distribution was tested by setting the holdup volume on each tray in the reaction zone to 0.549 m^3.

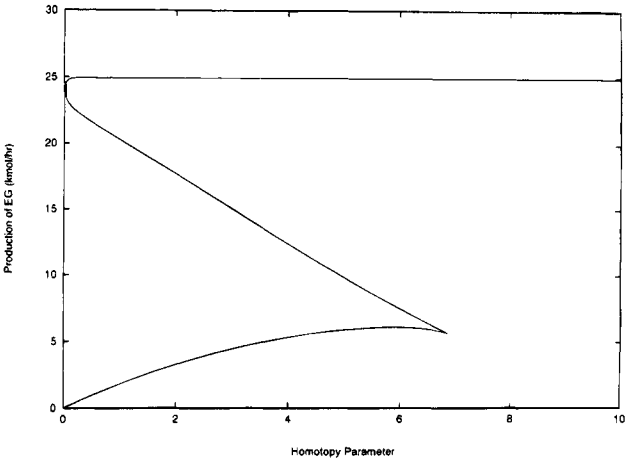

Figure 12. Homotopy curve for evenly distributed holdup volumes: ethylene glycol production versus λ_1.

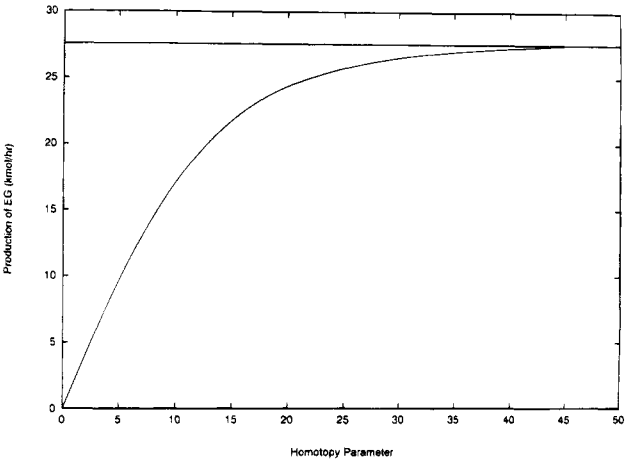

Figure 13. Homotopy curve for single reaction system: ethylene glycol production versus λ_1.

A plot of ethylene glycol production vs λ_1 for a uniform holdup distribution is given in Figure 12. Again there is no qualitative change in the number or form of multiplicities.

7.3. Multiple Reactions. The effect of the second reaction upon the number and form of the steady state multiplicities in the column was tested by removing the reaction and diethylene glycol compound from the model, increasing the water feed rate from 26.3 to 27.56 kmol/h, and repeating the homotopy study.

The water feed rate was increased so that water and oxide were fed to the column in a strict 1:1 ratio. The original column used a slight excess of ethylene oxide; this oxide reacted with ethylene glycol to form the unwanted byproduct DEG. The cusplike turning point occurred when all of the oxide had reacted. If the second reaction is removed from the model without increasing the water flow rate, then there will always be a slight excess of oxide. As a result, the reactive distillation homotopy curve may not leave the lower branch of the homotopy; the curve will not pass through the cusplike turning point and there will be no steady state multiplicities. Increasing the water feed removes an artificial constraint upon the number of multiplicities and the form of the homotopy curve.

Figure 13 shows a plot of the ethylene glycol production rate as a function of the homotopy parameter λ_1. Notice that the cusp point has moved from $\lambda_1 \approx 7$ to $\lambda_1 \approx 45$, and that the intermediate and upper branches of the homotopy curve seem to have merged into a single

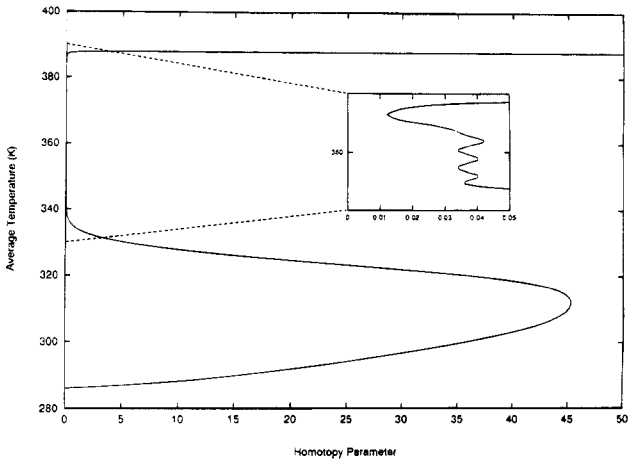

Figure 14. Homotopy curve for single reaction system: average column temperature versus λ_1.

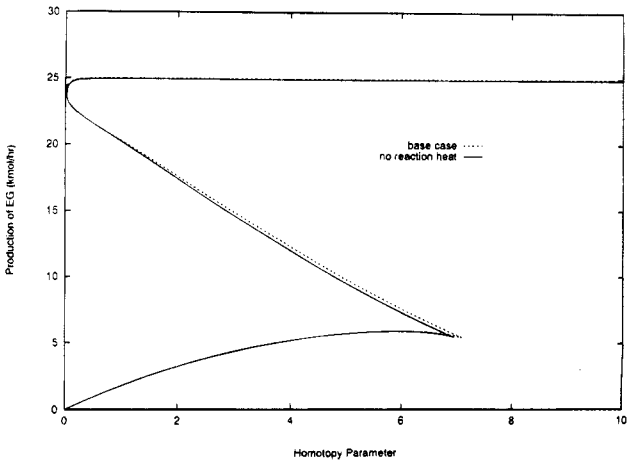

Figure 15. Homotopy curve for thermally neutral reaction system: ethylene glycol production versus λ_1.

horizontal line. The intermediate and upper steady states have not actually merged. There are still three steady states at high values of the holdup volume, and a large number of steady states at small values of the holdup volume. In the original system, the presence of a second reaction created a selectivity effect that made the steady state multiplicities easy to identify on an ethylene glycol production curve. When there is no second reaction there is no selectivity effect, but the dramatic multiplicities in the column temperature and composition profiles remain. This can be seen more clearly on a plot of the average column temperature (Figure 14).

7.4. Heat of Reaction. The ethylene glycol system involves highly exothermic reactions: the heat of the ethylene glycol reaction (−80 kJ/mol) is nearly twice of the heat of vaporization of water (40.6 kJ/mol). This is a plausible trigger for the multiplicities observed in the base case design, since large exothermic heats of reaction are known to cause multiplicities in CSTR's.

The effect of reaction heats in the ethylene glycol system was explored by artificially setting the heat of reactions to zero. The homotopy curve for this thermally neutral reaction system is shown in Figure 15. When there is no reaction heat, the column still has three steady states at large values of λ_1, and as many as nine steady states at small values of λ_1. Clearly, the heat of reaction has no significant effect upon the number and form of the multiplicities in the reactive distillation column.

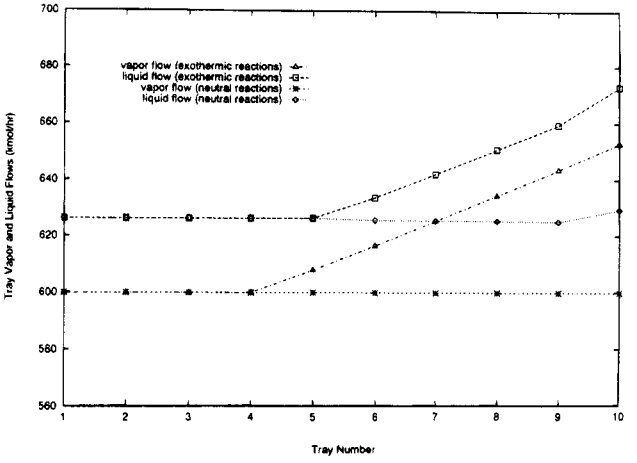

Figure 16. Effect of reaction heat on liquid and vapor profiles.

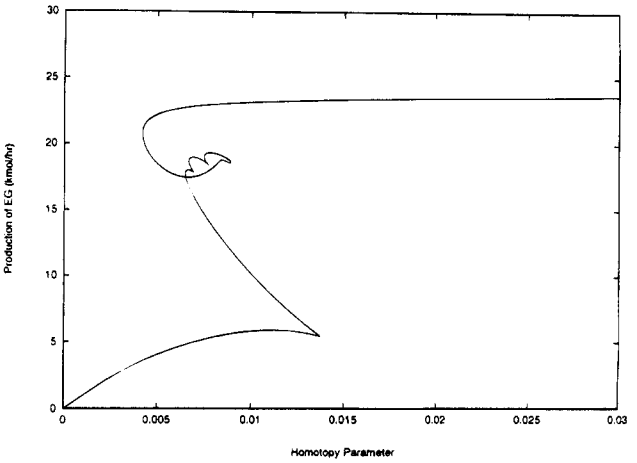

Figure 17. Homotopy curve for constant reaction rates: ethylene glycol production versus λ_1.

In this reactive distillation column, the exothermic heats of reaction only affect the profile of liquid and vapor flows, as shown in Figure 16. The heat of reaction has no effect on the temperature and composition profiles within the column.

7.5. Activation Energy. Another potential source of multiplicities is the coupling between the temperature profile and the extent of reaction via temperature-dependent kinetic rate constants.

This hypothesis was tested by setting the reaction rate of the ethylene glycol reaction to $16120x_{EO}x_W$ kmol/(m^3 h) and the reaction rate of the diethylene glycol reaction to $32460x_{EO}x_{EG}$ kmol/(m^3 h). These reaction rate expressions do not contain a temperature-dependence term, and so the reaction rate is decoupled from the column temperature profile.

The homotopy curve for this modified system is shown in Figure 17. Notice that while the scale of the curve has changed dramatically, the shape and multiplicity features of the curve remain. There is still a cusplike turning point at low production levels and a second region of multiplicity at high production levels. Clearly, the steady state multiplicities in the system do not arise from a coupling between vapor−liquid equilibria and temperature-dependent reaction rate terms.

7.6. Volatility Difference between Reactants. The base case analysis demonstrated that the ratio of oxide to water at specific points in the column varies dramatically from one steady state to another. The large difference between the boiling points of ethylene oxide and water means that the temperature profiles

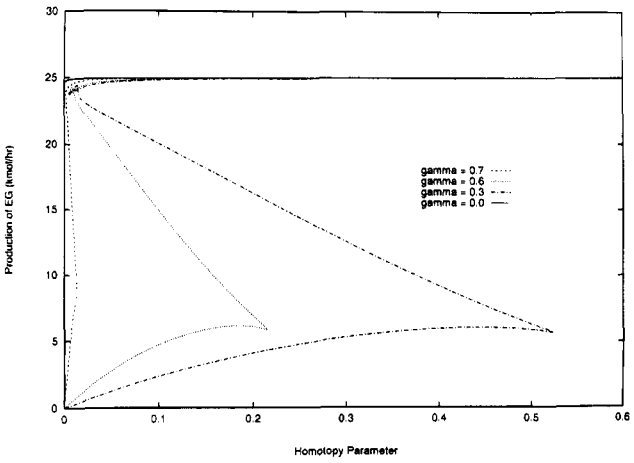

Figure 18. Homotopy curves for various feed volatilities: ethylene glycol production versus λ_1.

within the column will also vary dramatically from one steady state to another.

The effect of the volatility difference between reactants upon the steady state multiplicity of a distillation column was studied by artifically weighting the Antoine coefficients for ethylene oxide:

$$\mathbf{A}_{EO}^{eff} = \gamma \mathbf{A}_{EO} + (1 - \gamma)\mathbf{A}_{W} \tag{16}$$

when the weight γ equals 1, the vector of the effective Antoine coefficients for ethylene oxide equals the actual Antoine coefficients. When $\gamma = 0$, the effective Antoine coefficients for ethylene oxide equal the coefficients for water, and there is no volatility difference between ethylene oxide and water.

Figure 18 shows the effect of the volatility difference between the reactants upon the homotopy curve for $\gamma = 0$, 0.3, 0.6, and 0.7. As γ approaches zero, the scope of the large-scale multiplicity rapidly narrows and the small-scale multiplicities smooth out and disappear. At $\gamma = 0$, the homotopy curve has become single-valued and monotonic: the production rate of ethylene glycol increases continuously with increasing λ_1. The multiplicities in the reactive distillation column are clearly linked to the large volatility difference between ethylene oxide and water.

8. Discussion

The homotopy studies reported in this paper demonstrate that two types of steady state multiplicities can occur in an ethylene glycol reactive distillation column. The first type is a large-scale three-branch multiplicity that leads to three steady states in the optimal column. The second type is a complex switchbacking multiplicity that occurs at small holdup volumes. Because of these multiplicities, the column can have as many as nine distinctly different steady states.

The multiplicities did not arise from uneven distributions of the oxide feed or the reacting holdup volume. The presence of a second reaction created a selectivity effect that dramatized the multiplicities, but was not a dominant cause. The temperature dependence of the reaction rate constants has some effect upon the switchbacking multiplicity, and magnified *but did not cause* the large-scale three-branch multiplicity. Most surprisingly, the heat of reaction had no effect upon the number of multiplicities or the shape of the homotopy curve.

The combination of a bilinear reaction rate and a sharp volatility difference between the reactant feeds is the primary cause of the large-scale three-branch multiplicity, and a significant factor in the switchbacking multiplicities. When the Antoine's coefficients for ethylene oxide were set equal to the Antoine's coefficients for water, all multiplicities disappeared, and the production rate and temperature profile increased smoothly and monotonically with the holdup volume.

We propose the following explanation for the three-branch multiplicity. When there is no reaction, the ethylene oxide and water feeds fractionate within the column. The large volatility difference between oxide and water creates a distinctive column profile: the column is essentially full of oxide, there is almost no water anywhere within the column, the column temperature profile is flat, and the temperature everywhere in the column is close to the boiling point of ethylene oxide.

When this system is perturbed by introducing a reaction, the temperature and ethylene oxide composition profiles are essentially constant, and the primary reaction that produces ethylene glycol is pseudo-first-order in the water concentration. As the holdup volume increases, more and more of the water feed is consumed in the reaction. The production of ethylene glycol increases monotonically until all of the oxide *feed* has been consumed. During this phase, the internal reflux provided by distillation assures that the oxide concentration in the reaction zone remains high despite the increased consumption of oxide. This process creates the lower branch of the homotopy curve.

Once all of the oxide has been consumed, the column behaves differently. The column is still full of ethylene oxide, and the temperature within the reaction zone is still nearly constant and equal to the boiling point of ethylene oxide. However, there is no oxide in the bottom product. Water begins to supplant ethylene oxide in the vapor recycled into the reaction zone from the separation zone in the bottom of the column, and the water concentration in the reaction zone begins to increase.

The increasing water concentration in the reaction zone creates the cusplike turning point. This can be seen most clearly by considering the single reaction case. The overall extent of the first reaction is approximated by

$$\xi_1 = \lambda_1 k W x_{EO} x_W \tag{17}$$

Here, ξ_1 is the extent of the first reaction, λ_1 is the homotopy parameter, and k, W, x_{EO}, and x_W are kinetic rate constants, average holdups, oxide concentrations, and water concentrations. W is constant, the extent of reaction near the cusp point is nearly constant, and since the temperature in the reaction zone is nearly constant, k is nearly constant. In the single reaction case, ξ_1 is constant near the turning point and equal to the feed rate of ethylene oxide. Consequently, one can say that

$$\lambda_1 x_{EO} x_W \approx \text{constant} \tag{18}$$

Taking the partial derivative of this expression with respect to the water concentration yields an approximate expression for the change in λ_1 near the cusp point:

$$\frac{\partial \lambda_1}{\partial x_W} = -\lambda_1 \left[\frac{1}{x_{EO}} \frac{\partial x_{EO}}{\partial x_W} + \frac{1}{x_W} \right] \tag{19}$$

Since the products are significantly heavier than the reactants, we can say that

$$x_{EO} + x_w \approx 1$$

so that

$$\frac{\partial x_{EO}}{\partial x_W} \approx -1$$

With this approximation, eq 19 becomes

$$\frac{\partial \lambda_1}{\partial x_W} = -\lambda_1\left[\frac{1}{x_W} - \frac{1}{x_{EO}}\right] \tag{20}$$

Note that x_{EO} is approximately 1 within the reactive zone of the column, and $x_W \approx 0$. The homotopy parameter *decreases* as the concentration of water in the reaction zone increases:

$$\frac{\partial \lambda_1}{\partial x_W} = -\lambda_1\left[\frac{1}{x_W} - 1\right] < 0 \tag{21}$$

Initially, before the oxide is completely consumed, there is almost no water in the vapor boilup. The concentration of water within the reaction zone decreases steadily while the homotopy parameter increases, forming the lower branch of the homotopy curve. Once the oxide has been consumed, the vapor boilup begins to return water vapor to the reaction zone, and the water concentration within the zone begins to increase. The homotopy parameter must decrease, creating a turning point and the intermediate branch of the homotopy curve.

The transition between the upper branch and the intermediate branch occurs in a series of rapid switchbacks. These switchbacks create a small range of holdup volumes with a large number of steady states. Each switchback is marked by a dramatic change in temperature and composition on one or two trays in the reaction zone. The multiplicities in the switchbacking region were quite susceptible to changes in the activation energy and volatility difference. We note that these multiplicities occur at very small holdup volumes and consequently they are not physically significant for the glycol column presented in section 2. However, we see no reason why this type of multiplicity would be limited to small holdup volumes in other systems, and should not be dismissed completely.

In some ways the upper branch of the homotopy curve is a mirror image of the lower branch. Here, the reaction zone is full of water, the temperature within the zone is constant and approximately equal to the boiling point of water, and the reactions are pseudo-first-order in the oxide concentration.

It is interesting to compare these results with previous published studies. Nijhuis et al. (1993) have reported finding two steady states during steady state simulations of a methyl *tert*-butyl ether (MTBE) column. MTBE is formed from methanol and isobutene:

$$CH_3OH + (CH_3)_2CCH_2 \rightarrow (CH_3)COCH_3$$

The forward reaction producing MTBE has bilinear reaction rates; moreover, isobutene, with a normal boiling point of −7 °C, is considerably more volatile than methanol, which boils at 64.7 °C. Nijhuis et al. (1993) attribute the multiplicities in the MTBE system to the temperature effects on the reversible reaction, but the volatility difference between the reactants may be a viable alternative explanation.

Chang and Seader (1988) applied homotopy continuation methods to a reactive distillation column producing ethyl acetate from ethanol and acetic acid. This system has bilinear reaction rates, and the feeds, ethanol and acetic acid, have relatively close boiling points (78 and 118 °C, respectively). Chang and Seader found a unique steady state, suggesting that the volatility difference between the reactants was not large enough to create multiplicities.

9. Conclusions

A series of computational experiments were performed on a reactive distillation column producing ethylene glycol from ethylene oxide and water. The experiments used homotopic continuation to test for steady state multiplicities under a range of conditions. The reactive distillation column showed two distinct types of multiplicities: a large-scale three-branch multiplicity and small-scale switchbacking multiplicities. The column has three steady states at normal holdup volumes, and could have as many as nine steady states at small holdup volumes. These steady states differed by dramatic changes in the composition and temperature profiles within the column.

The computational studies showed that feed and holdup volume distributions had little effect on the number of steady state multiplicities. Surprisingly, the heat of reaction had no effect whatsoever on the number of multiplicities or the shape of the homotopy curve. The multiplicities were not caused by the presence of a second reaction. However, the presence of a second reaction did introduce a selectivity effect that made the ethylene glycol production rate sensitive to the column multiplicities.

The activation energy of the reactions clearly affected the size of the multiplicity region, but did not change the three-branch multiplicity. Instead, the three-branch multiplicities appear to arise from volatility differences between the reactants and the bilinear structure of the reaction rates. The lower turning point of this multiplicity occurs when there is no ethylene oxide in the bottoms stream of the column. This is accompanied by an increasing amount of water in the vapor boilup, which in turn triggers the turning point. The upper turning point is acheived through a switchbacking multiplicity that generates a large number of steady states. This switchbacking multiplicity is more complex than the large-scale three-branch multiplicity and is affected by both the reaction kinetics and the volatility difference between the reactants.

Acknowledgment

The authors gratefully acknowledge financial support from the National Science Foundation under Grant CTS-9309172.

Notation

$\mathbf{A}_B$ = basis matrix
$\mathbf{A}$ = vector of Antoine coefficients
$\mathbf{A}^{eff}$ = vector of Antoine coefficients
$\mathbf{A}_N$ = nonbasic matrix
$\mathbf{c}$ = vector of constants
$\mathbf{f}(\mathbf{x})$ = vector of nonlinear functions
f_j = kinetic equation for chemical reaction j

$\mathbf{g}(\mathbf{x})$ = vector of nonlinear functions
$F_{i,k}$ = feed rate of component i from tray k
$h(\mathbf{x})$ = nonlinear objective function
$\mathbf{H}(\mathbf{x},\lambda)$ = homotopy function
H_{vap} = heat of vaporization at boiling point
ΔH_j = heat of reaction j
I = maximum number of components
J = maximum number of chemical reactions
$K_{i,k}$ = vapor–liquid equilibrium coefficient
L_k = liquid stream from tray k
N = maximum number of trays
T_k = temperature on tray k
V_k = vapor stream from tray k
W_k = holdup volume on tray k
$\mathbf{x}$, $\mathbf{x}_0$ = vectors of real variables
$\mathbf{x}_B$ = basic variables
$\mathbf{x}_N$ = nonbasic variables
$x_{i,k}$ = mole fraction of component i on tray k

Greek Letters

β = reboil ratio
γ = weight of Antoine coefficients
λ, λ_1 = homotopy parameters
ϱ = penalty parameter
$\xi_{j,k}$ = extent of chemical reaction j on tray k
$\nu_{i,j}$ = stoichiometric coefficient of component i in reaction j

Subscripts

EO = ethylene oxide
i = component index
j = chemical reaction index
k = column tray index
W = water

Appendix

Reduced gradient algorithms are iterative approaches for solving constrained nonlinear optimization problems of the form

$$\min_x h(\mathbf{x}) \tag{22}$$

subject to

$$\mathbf{f}(\mathbf{x}) = \mathbf{c} \tag{23}$$

$$\mathbf{x} \in R^n \tag{24}$$

Here, $\mathbf{x}$ is a vector of decision variables, $h(\mathbf{x})$ is an objective function, and $\mathbf{f}(\mathbf{x}) = \mathbf{c}$ is an m-dimensional vector of nonlinear equality constraints.

At each iteration of a reduced gradient algorithm, the nonlinear constraints are replaced by first-order Taylor series expansions:

$$\min_{\mathbf{x}} h(\mathbf{x}) + \varrho[\mathbf{f}(\mathbf{x}_0) + \nabla \boldsymbol{f}\cdot(\mathbf{x}-\mathbf{x}_0) - \mathbf{f}(\mathbf{x})]^T\cdot[\mathbf{f}(\mathbf{x}_0) + \nabla \boldsymbol{f}\cdot(\mathbf{x}-\mathbf{x}_0) - \mathbf{f}(\mathbf{x})] \tag{25}$$

subject to

$$\mathbf{f}(\mathbf{x}_0) + \nabla \mathbf{f}\cdot(\mathbf{x}-\mathbf{x}_0) = \mathbf{c} \tag{26}$$

Here, the penalty term $\varrho[\mathbf{f}(\mathbf{x}_0) + \nabla \mathbf{f}\cdot(\mathbf{x} - \mathbf{x}_0) - \mathbf{f}(\mathbf{x})]^T\cdot[\mathbf{f}(\mathbf{x})]^T\cdot[\mathbf{f}(\mathbf{x}_0) + \nabla \mathbf{f}\cdot(\mathbf{x} - \mathbf{x}_0) - \mathbf{f}(\mathbf{x})]$ has been added to the objective in order to prevent the optimization problem from straying too far from the linearization point.

The variables $\mathbf{x} - \mathbf{x}_0$ in this problem are partitioned into m basic variables $\mathbf{x}_B$ and $n - m$ nonbasic variables $\mathbf{x}_N$. The Jacobian matrix $\nabla \boldsymbol{f}$ is partitioned into a square $m \times m$ basis matrix $\boldsymbol{A}_B$ and a nonsquare matrix $\boldsymbol{A}_N$, giving the following transformed optimization problem:

$$\min_{\mathbf{x}_B,\mathbf{x}_N} h(\mathbf{x}_B,\mathbf{x}_N) + \varrho[\boldsymbol{A}_B\mathbf{x}_B + \boldsymbol{A}_N\mathbf{x}_N + \mathbf{f}(\mathbf{x}_0) - \mathbf{f}(\mathbf{x}_B,\mathbf{x}_N)]^T\cdot[\boldsymbol{A}_B\mathbf{x}_B + \boldsymbol{A}_N\mathbf{x}_N + \mathbf{f}(\mathbf{x}_0) - \mathbf{f}(\mathbf{x}_B,\mathbf{x}_N)] \tag{27}$$

subject to

$$\boldsymbol{A}_B\mathbf{x}_B + \boldsymbol{A}_N\mathbf{x}_N = \mathbf{c} - \mathbf{f}(\mathbf{x}_0) \tag{28}$$

The linear constraints are solved to give the basic variables in terms of the nonbasic variables:

$$\mathbf{x}_B = \boldsymbol{A}_B^{-1}\cdot[\mathbf{c} - \mathbf{f}(\mathbf{x}_0) - \boldsymbol{A}_N\mathbf{x}_N] \tag{29}$$

These variables can be substituted into the objective, giving an unconstrained optimization problem:

$$\min_{\mathbf{x}_N} h(\boldsymbol{A}_B^{-1}\cdot[\mathbf{c}-\mathbf{f}(\mathbf{x}_0)-\boldsymbol{A}_N\mathbf{x}_N],\mathbf{x}_N) + [\mathbf{c} - \mathbf{f}(\boldsymbol{A}_B^{-1}(\mathbf{c}-\mathbf{f}(\mathbf{x}_0)-A_N\mathbf{x}_N),\mathbf{x}_N)]^T\cdot[\mathbf{c} - \mathbf{f}(\boldsymbol{A}_B^{-1}(\mathbf{c}-\mathbf{f}(\mathbf{x}_0)-A_N\mathbf{x}_N),\mathbf{x}_N)] \tag{30}$$

This unconstrained problem is solved to give the optimal values of the nonbasic variables $\mathbf{x}_N$, which in turn can be used as a starting point $\mathbf{x}_0$ for the next iteration for the algorithm.

If the original system of nonlinear constraints is square, there are no nonbasic variables, and the basic variables are uniquely defined by

$$\mathbf{x}_B = \mathbf{x}_0 + \nabla \boldsymbol{f}^{-1}\cdot[\mathbf{f}(\mathbf{x}_0) - \mathbf{c}] \tag{31}$$

Each iteration of the reduced gradient algorithm computes a new value of the basis vector. The routine stops when $\mathbf{f}(\mathbf{x}_B) = \mathbf{c}$. Thus, when there are no degrees of freedom, the optimization routine devolves into a Newtonian code for solving systems of nonlinear equations.

It should be noted that bifurcations of the function set $\mathbf{f}(\mathbf{x}) = \mathbf{c}$ occur at singular points where the Jacobian matrix $\nabla \boldsymbol{f}$ is indeterminate. At these points, the Jacobian matrix cannot be inverted. When there are no degrees of freedom, the Jacobian matrix equals the basis matrix, and bifurcation points of the function set $\mathbf{f}(\mathbf{x}) = \mathbf{c}$ will be detected by the reduced-gradient optimization routine as singularities in the basis matrix.

Literature Cited

Alexander, J. C.; Yorke, J. A. The homotopy continuation method: Numerically implementable topological procedures. *Trans Am. Math. Soc.* **1978**, *242*, 313–323.

Backus, A. A. "Continuous Process for the Manufacture of Ethers". US Patent 1,400,849, 1921.

Barbosa, D.; Doherty, M. F. "Design and Minimum-Reflux Calculations for Single-Feed Multicomponent Reactive Distillation Columns". *Chem. Eng. Sci.* **1988a**, *43*, 1523–1537.

Barbosa, D.; Doherty, M. F. "Design and Minimum-Reflux Calculations for Single-Feed Multicomponent Reactive Distillation Columns". *Chem. Eng. Sci.* **1988b**, *43*, 2377–2389.

Brooke, A.; Kendrick, D.; Meeraus, A. *GAMS: A Users Guide*; Scientific Press: Redwood City, CA, 1988.

Carra, S.; Morbidelli, M.; Santacesaria, E.; Buzzi, G. "Synthesis of Propylene Oxide from Propylene Chlorohydrins—II". *Chem. Eng. Sci.* **1979**, *34*, 1133–1140.

Chang, Y. A.; Seader, J. D. "Simulation of Continuous Reactive Distillation by Homotopy-Continuation Methods". *Comput. Chem. Eng.* **1988**, *12*, 1243–1255.

Ciric, A. R.; Gu, G. "Synthesis of Nonequilibrium Reactive Distillation Processes via Mixed Integer Nonlinear Programming". *AIChE J.* **1994**, in press.

Doherty, M. F.; Buzad, G. "Reactive Distillation by Design". *Chem. Eng. Res. Des.* **1992**, *70*, 448–458.

Izarraraz, A.; Bentsen, G. W.; Anthony, R. G.; Holland, C. D. "Solve More Distillation Problems. Part 9: When Chemical Reactions Occur". *Hydrocarbon Process.* **1980**, *59*, 195–203.

Jacobs, R.; Krishna, R. "Multiple solutions in Reactive Distillation for Methyl *tert*-Butyl Ether Synthesis". *Ind. Eng. Chem. Res.* **1993**, *32*, 1706–1709.

Komatsu, H. "Application of the Relaxation Method for Solving Reacting Distillation Problems". *J. Chem. Eng. Jpn.* **1977**, *10*, 200–205.

Komatsu, H.; Holland, C. D. "A New Method of Convergence for Solving Reactive Distillation Problems". *J. Chem. Eng. Jpn.* **1977**, *10*, 292–297.

Kuno, M.; Seader, J. D. "Computing all Real Solutions to Systems of Nonlinear Equations with a Global Fixed-Point Homotopy". *Ind. Eng. Chem. Res. 27*, 1320–1329.

Luyben, W. L. "Design and Control of Coupled Reactor/Column Processes". Presented at the AIChE Annual Meeting, St. Louis, MO, 1993; paper 195g.

Morbidelli, M.; Varma, A.; Aris, R. "Reactor Steady State Multiplicity and Stability". In *Chemical Reaction and Reactor Engineering*; Carberry, J. J., Varma, A., Eds.; Marcel Dekker: New York, 1987; pp 973–1054.

Nelson, P. A. "Countercurrent Equilibrium Stage Separation with Reaction". *AIChE J.* **1971**, *17*, 1043–1049.

Nijhuis, S. A.; Kerkhof, F. P. J. M.; Mak, A. N. S. "Multiple Steady States during Reactive Distillation of Methyl *tert*-Butyl Ether". *Ind. Eng. Chem. Res.* **1993**, *32*, 2767–2774.

Pisarenko, Y. A.; Epifanova, O. A.; Serafimov, L. A. "Steady States for a Reaction Distillation Column with One Product Stream". *Theor. Found. Chem. Eng.* **1988**, *21*, 281–286.

Suzuki, I.; Yagi, H.; Komatsu, H.; Hirata, M. "Calculation of Multicomponent Distillation Accompanied By Reaction". *Chem. Eng. Commun.* **1971**, *16*, 91–108.

Tirney, J. W.; Riquelme, G. D. "Calculation Methods for Distillation Systems with Reaction". *Chem. Eng. Commun.* **1982**, *16*, 91–108.

Ung, S.; Doherty, M. F. "Synthesis of Reactive Distillation Systems with Multiple Reactions". Presented at the AIChE Annual Meeting, St. Louis MO, 1993; paper 152b.

Venkataraman, S.; Chan, W. K.; Boston, J. F. "Reactive Distillation Using ASPEN PLUS". *Chem. Eng. Prog.* **1990**, 45–54.

Wayburn, T. L.; Seader, J. "Homotopy Continuation Methods for Computer Aided Design". *Comput. Chem. Eng.* **1990**, *11*, 7–25.

Xu, X.; Chen, H. "Simulation of Distillation Processes with Reactions In Series". *J. Chem. Ind. Eng.* **1988**, *3*, 57–69.

Received for review February 7, 1994
Revised manuscript received July 13, 1994
Accepted July 19, 1994[⊗]

[⊗] Abstract published in *Advance ACS Abstracts,* October 1, 1994.